



HAL
open science

Transverse Particle Trapping Using Finite Bessel Beams Based on Acoustic Metamaterials

Xudong Fan, Yifan Zhu, Zihao Su, Ning Li, Xiaolong Huang, Yang Kang, Can Li, Chunsheng Weng, Hui Zhang, Weiwei Kan, et al.

► **To cite this version:**

Xudong Fan, Yifan Zhu, Zihao Su, Ning Li, Xiaolong Huang, et al.. Transverse Particle Trapping Using Finite Bessel Beams Based on Acoustic Metamaterials. *Physical Review Applied*, 2023, 19 (3), pp.034032. 10.1103/PhysRevApplied.19.034032 . hal-04271543

HAL Id: hal-04271543

<https://hal.science/hal-04271543>

Submitted on 6 Nov 2023

HAL is a multi-disciplinary open access archive for the deposit and dissemination of scientific research documents, whether they are published or not. The documents may come from teaching and research institutions in France or abroad, or from public or private research centers.

L'archive ouverte pluridisciplinaire **HAL**, est destinée au dépôt et à la diffusion de documents scientifiques de niveau recherche, publiés ou non, émanant des établissements d'enseignement et de recherche français ou étrangers, des laboratoires publics ou privés.

Transverse Particle Trapping Using Finite Bessel Beams based on Acoustic Metamaterials

Xudong Fan,^{1,*} Yifan Zhu,² Zihao Su,² Ning Li,¹ Xiaolong Huang,¹ Yang Kang,¹ Can Li,¹ Chunsheng Weng,¹ Hui Zhang,^{2,†} Weiwei Kan,^{3,‡} and Badreddine Assouar^{4,§}

¹*National Key Laboratory of Transient Physics, Nanjing University of Science and Technology, Nanjing 210094, China*

²*Jiangsu Key Laboratory for Design and Manufacture of Micro-Nano Biomedical Instruments, School of Mechanical Engineering, Southeast University, Nanjing 211189, China*

³*School of Science, MIT Key Laboratory of Semiconductor Microstructure and Quantum Sensing, Nanjing University of Science and Technology, Nanjing 210094, China*

⁴*Université de Lorraine, CNRS, Institut Jean Lamour, F-54000 Nancy, France.*

(Dated: November 6, 2023)

We investigate the transverse trapping force acting on a small particle on/off the central axis of zero-order finite Bessel beams. Combining the simulated fields with the Gorkov force potential, the transverse trapping behaviors on small objects are analyzed, and the reversal of the trapping behaviors is recovered when varying the paraxiality parameter of the Bessel beam. The results prove the possibility of using axisymmetric Bessel beams to trap both dense and stiff particles as well as light and soft ones. The particles can be trapped at the maximum central pressure in the main lobe and also the maximum pressure of the other transverse locations. A lossy acoustic metastructure with the ability to decouple the phase and amplitude modulations is used to generate the desired sound field, which is used to trap a foam ball as an example. Our research opens a promising avenue to design and develop simplified acoustic tweezers.

I. INTRODUCTION

Acoustic waves, as one of the most important forms in the classical wave system, play a significant role in the development of science and technology. When an object is placed in an acoustic field, there exists an acoustic radiation force acting on it. The force originates from the momentum transfer from the field to the object due to the scattering, reflection, and absorption. The acoustic radiation force acts throughout the object, but owing to the overall momentum conservation, the radiation force can be reduced to an integration of the time-averaged momentum-flux tensor over an arbitrary closed surface enclosing the whole object. [1] Acoustic radiation forces have been studied for a long time in regards to the sound waves of different forms. [2–17] The trapping behaviors generated by standing waves on small objects (object sizes are much smaller than the wavelength) have been well understood, [2] where relatively light and soft particles (like droplets) are trapped to the pressure maximum (anti-node), yet relatively dense and stiff particles (like elastic objects) would be trapped to pressure minimum (node). On the other hand, the recent studies on acoustic radiation forces based on non-diffracting beams [4–6, 14, 15, 18–20] have predicted the possibility for particle manipulations with more flexibility. However, in practical situations and applications, non-diffracting beams, such as acoustic

Bessel beams, would be difficult to generate by a finite source due to relatively complex transverse structures. Hence, it is significantly important to precisely generate and control the desired sound field. The conventional method would use a speaker/transducer array connected with a multi-signal generator, and then the desired sound field could be generated by adjusting the signal for each speaker/transducer individually. [10] Sound field manipulation based on such an active method has the advantage of flexibility, yet as the complexity of the array system increases, the cost, and the complexity of the signal processing will also increase. Hence, it is desired to realize precise field manipulations with simplicity and low cost. Recently, the emergence and the rapid development of acoustic metamaterials [21] open a field in acoustics, and also provide an approach for field manipulations. [22–39] Acoustic metamaterials can achieve extraordinary properties and phenomena, which natural materials would be difficult to achieve, such as negative refraction/reflection, [22, 23] cloaking, [40–44] hologram, [11, 36, 45–47] and specific field generations. [22, 24, 32]

In this work, we investigate the transverse acoustic radiation force generated by finite Bessel beams based on acoustic metamaterials. The transverse trapping behaviors of a small particle on/off the central axis of the Bessel beams are studied numerically and experimentally. A lossy acoustic metastructure, capable of decoupling the phase and amplitude modulations, is designed to generate the desired Bessel field, which is then used to trap a small foam ball to the beam center as an example. Our work gains insight into some unusual and unique trapping behaviors, which will help the further study of particle manipulations using acoustic radiation forces and acoustic Bessel fields.

* fanxudong@njust.edu.cn

† seuzhanghui@seu.edu.cn

‡ kan@njust.edu.cn

§ badreddine.assouar@univ-lorraine.fr

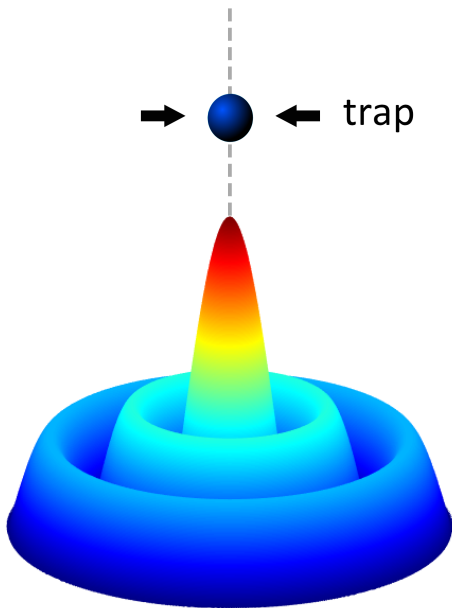


FIG. 1. Illustration of transverse particle trapping by acoustic Bessel beams.

II. NUMERICAL SIMULATION

We consider here a particle within a finite axisymmetric Bessel beam [Fig. 1], which can be approximately considered as a non-diffracting beam within a certain transverse radius and a certain propagating distance. The pressure field within such regions $\text{Re}[p(\mathbf{r}, t)]$ (Re denotes the real part) of the finite zero-order Bessel beams propagating along a z axis is given by,

$$p(\mathbf{r}, t) = p_0 J_0(\mu\rho) \exp(i\kappa z - i\omega t), \quad (1)$$

where p_0 is a real-valued amplitude, J_0 is zero-order Bessel function, $\mathbf{r}(\rho, \phi, z)$ is the field point in cylindrical coordinates, and the transverse wavenumber μ and axial wavenumber κ are related to the total wavenumber $k = \sqrt{\mu^2 + \kappa^2} = \omega/c_0$ (c_0 is sound speed in the surrounding media) through a paraxial parameter β with $\mu = k \sin \beta$, and $\kappa = k \cos \beta$.

The force potential U is then obtained based on the simulated pressure p and velocity fields \mathbf{v} , [2] i.e.,

$$U = (\pi a^3/3)[f_1 |p|^2 / (\rho_0 c_0^2) - (3/2) f_2 \rho_0 |\mathbf{v}|^2], \quad (2)$$

where a is the radius of the object, ρ_0 and c_0 are the mass density and the sound speed of the background medium, and f_1 and f_2 are the monopole and dipole factors depending on the mass density ratio and bulk modulus ratio between the object and the surrounding medium. [15] Here, rigid particles with $f_1 = 1 = f_2$ were used in the calculation since for most solid objects, the density and bulk modulus are much larger than the background medium, air, so the results here are applicable to most elastic objects.

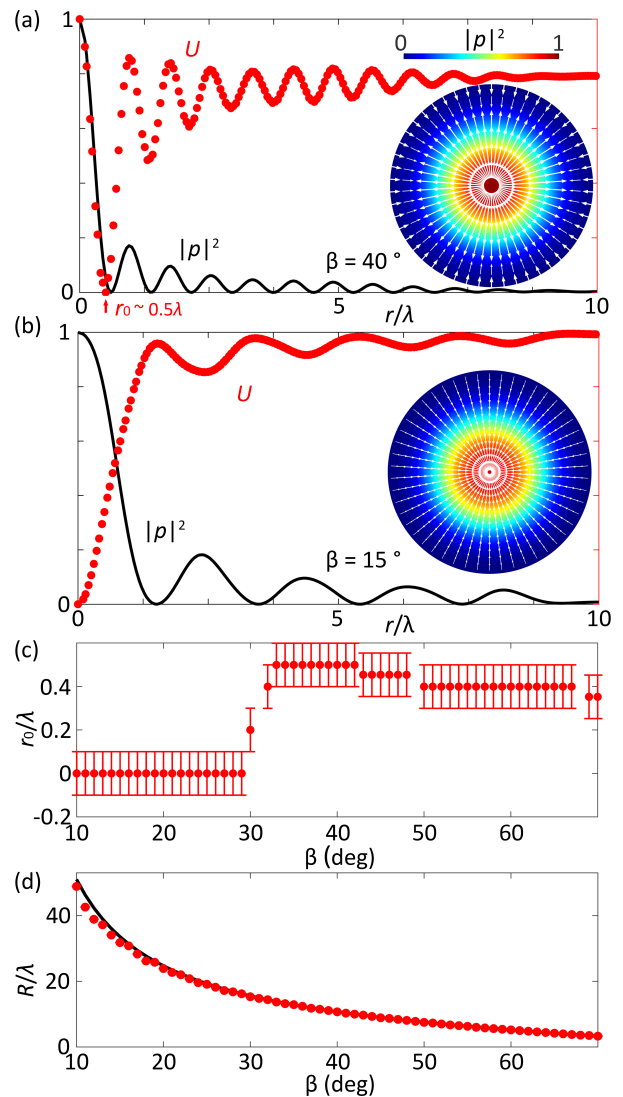


FIG. 2. Reversal of transverse particle trapping behaviors when reducing the angle from (a) $\beta = 40^\circ$ to (b) $\beta = 15^\circ$. Black solid lines: normalized squared pressure, $|p|^2$, at $z = 3\lambda$; red dots: normalized force potential U computed from Eq. (2) based on the simulated pressure and velocity fields. Insets: two-dimensional normalized squared pressure (color plots) and the corresponding radiation forces (white arrows). (c) Variation of the first trapping location r_0 near the beam axis. Transition angle happens at $\beta \sim 29^\circ$. (d) Spatial range R for approximated Bessel beams from a finite sound source. Red dots: simulated results obtained based on the -3dB location in the z direction; black line: curve fitting, $R \approx 0.9H/\tan \beta$ with H being the half length of the finite source.

We first simulate the sound field of the finite zero-order Bessel beam with $\beta = 40^\circ$ [see Fig. 2(a)]. The red dots show the variation of the force potential [2] U [Eq. (2)] along the transverse location r/λ with λ being the wavelength, and the black solid line shows the corresponding sound pressure. Particles will be trapped to the local potential minimum, hence, for this case,

121 the rigid particle cannot be trapped to the pressure
 122 maximum at the beam center ($r = 0$), which agrees with
 123 the previous conclusion from the standing fields. [2] In
 124 addition, we find that for the off-axis transverse locations
 125 ($r > 0$), the force potential minimum coincides with the
 126 corresponding pressure minimum (or at most with a little
 127 shift), where the particles can be trapped. In particular,
 128 the nearest trapping location to the beam center for this
 129 case is at $r_0 \sim 0.5\lambda$, which is useful for trapping particles
 130 [see Inset for the two-dimensional pressure profile (color
 131 plot) and the radiation forces computed based on the
 132 force potential, i.e., $\mathbf{F} = -\nabla U$ (white arrows)]. However,
 133 when the angle β is reduced to be, for example, 15°
 134 [see Fig. 2(b)], the trapping behavior becomes different.
 135 Rigid particles will be instead trapped to the central
 136 pressure maximum [see white arrows in Inset for the
 137 radiation force], and in addition, almost all the potential
 138 minimum along the transverse location corresponds to
 139 the pressure maximum, where the rigid particle can be
 140 trapped. Comparing Fig. 2(a) and (b), one can find
 141 that for a large β [see (a)], there exist more potential
 142 minima at the same transverse distance, so the spatial
 143 resolution for the trapping will be improved. In addition,
 144 the transverse radiation force for a large β would be larger
 145 due to the large gradient of the force potential.

146 Here, the simulations were conducted in a
 147 two-dimensional axisymmetric model using the
 148 commercial software, COMSOL MULTIPHYSICS.
 149 The size of the computation domain is 10λ in radius and
 150 50λ in the z direction. Radiation boundaries were used
 151 to eliminate the reflection. Maximum mesh size was set
 152 to be $\lambda/10$ to obtain precise and accurate sound fields.
 153 The source is located at $z = 0$ and the background
 154 medium is air with the density of 1.21 kg/m^3 and the
 155 sound speed of 343 m/s .

156 We have numerically observed the reversal of the
 157 transverse trapping behaviors for rigid particles on the
 158 central beam axis ($r = 0$) as the angle β is reduced,
 159 which recovers the previous theoretical prediction for the
 160 ideal Bessel beams. [15] In order to examine the exact
 161 transition angle β for finite Bessel beams, a series of
 162 simulations were conducted for β from 10° to 70° . The
 163 nearest trapping location to the beam center is examined
 164 as a function of β [see Fig. 2(c)]. From the results, the
 165 trapping location first increases and then decreases as the
 166 angle β increases. The transition angle happens around
 167 $\beta \sim 29^\circ$, agreeing with the predicted value $\beta \sim 28^\circ$ in
 168 Fan and Zhang [15] within tolerance. The explanation of
 169 the reversal has been interpreted by the contribution of
 170 axial velocity to the force potential and by momentum
 171 projection therein.

172 Like plane waves, an ideal Bessel beam cannot be
 173 created since it requires an infinitely large source and also
 174 an infinite amount of energy. Hence, the approximated
 175 Bessel beams only exist within a certain spatial range.
 176 We examine the relationship between the approximated
 177 spatial range R with the angle β [see red dots in
 178 Fig. 2(d)], where the spatial range R for each angle

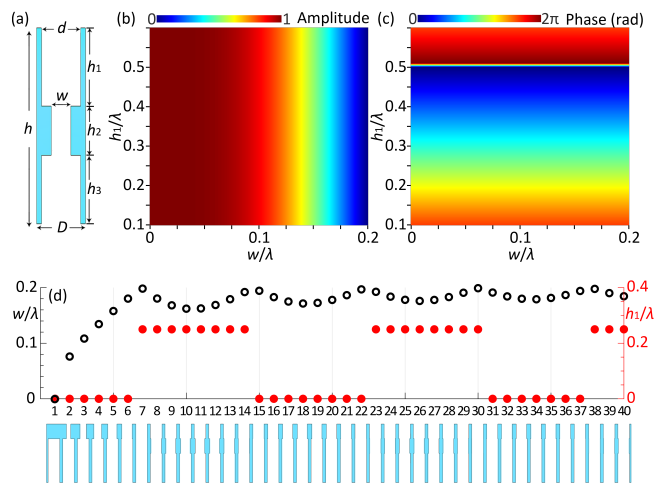


FIG. 3. (a) Illustration of one element of the artificial structure. Parameters are chosen as $h = \lambda$, $D = 0.25\lambda$, $d = 0.8D$, $h_2 = 0.5\lambda$, and $h = h_1 + h_2 + h_3$. λ is the wavelength. By adjusting the geometry parameters w and h_1 , (b) the amplitude and (c) the phase of the reflected field could be modulated separately [Eq. (4)]. (d) The artificial structure used in the simulation for $\beta = 15^\circ$, and the corresponding geometry parameters w (black circles) and h_1 (red dots) for the 40 elements.

179 β takes the location of -3dB along the propagating z
 180 direction. The relation between the spatial range R and
 181 the angle β for a finite source is roughly

$$R \approx 0.9H / \tan \beta \quad (3)$$

182
 183 with H being the half length of the source. Based on
 184 Eq. (3), the field can be approximately considered as
 185 a Bessel field within the allowable spatial range R for
 186 a given β and a source size H , and the Bessel beam
 187 with a small β could trap particles from a relatively long
 188 distance from the source.

189 III. EXPERIMENTAL REALIZATION

190 The desired acoustic Bessel beams could be generated
 191 using acoustic metamaterials. There usually exist
 192 relatively complex couplings between the amplitude
 193 and the phase of the reproduced sound field by the
 194 sophisticated artificial structure, and the conventional
 195 phase-only modulated metamaterials generally ignore the
 196 error caused by the unavoidable amplitude variation.
 197 Hence, acoustic metamaterials with the ability of
 198 decoupling the phase and amplitude modulations are
 199 preferred here.

200 In this work, a lossy acoustic metastructure is used
 201 to generate an acoustic Bessel beam with $\beta = 15^\circ$ [see
 202 Fig. 3(a)] for the cross-section of one element in the
 203 structure]. [36] This structure can achieve the decoupled

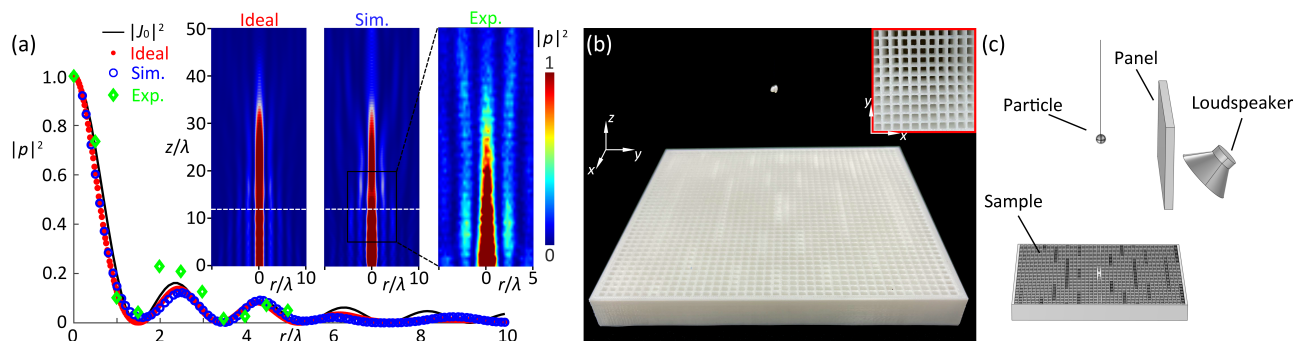


FIG. 4. Particle manipulations using finite Bessel beams. (a) Measured and simulated fields generated by the metastructure with the results compared with an ideal continuous distributed source. Comparison of the field profile $|p|^2$ at $z = 12\lambda$ (white dashed lines). J_0 is the zero-order Bessel function. (b) Experimental photo of the transverse particle trapping using acoustic metamaterials, where a foam ball is trapped at the center of the Bessel beam. The size of the sample is $20 \times 20 \times 2 \text{ cm}^3$, and the diameter of the foam ball is $\sim 2 \text{ mm}$. Inset: zoom-in photo of the sample. (c) Illustration of the experimental setup.

204 modulation of the amplitude A and the phase Φ , [36] i.e.,

$$205 \quad A = \frac{d^4 - w^4}{d^4 + w^4}, \Phi = -\frac{4\pi h_1}{\lambda}. \quad (4)$$

206 The decoupled modulation of the amplitude and the
207 phase allows for all the combinations in their full
208 parameter ranges [that is, $A \in [0, 1]$ and $\Phi \in [0, 2\pi]$; see
209 Fig. 3(b) and (c)], which is necessary to generate acoustic
210 Bessel beams in our case. The viscosity effect of the
211 metastructure here can be ignored since the boundary
212 layer thickness is much smaller than the width of the
213 elements. [48, 49] The cross-section of the structure and
214 the corresponding geometry parameters w and h_1 for the
215 40 elements are shown in Fig. 3(d), which would be used
216 to generate an zero-order Bessel beam with $\beta = 15^\circ$.

217 The measured and simulated fields $|p|^2$ generated via
218 the acoustic metastructure are shown in Fig. 4(a). The
219 results are further compared with the field generated by
220 an ideal continuously distributed Bessel source of the
221 same size. We have examined the transverse profile of
222 the field at $z = 12\lambda$ (white dashed lines). From the
223 results, one can find the fields generated via the acoustic
224 metastructure (green diamonds and blue circles) agree
225 pretty well with the ideal source of the same size (red
226 dots), and both of them follow the squared zero-order
227 Bessel function (black solid line). Hence, with the aid of
228 this structure, the zero-order Bessel beam is effectively
229 generated and can be utilized for particle manipulations.

230 As an example, the transverse particle trapping behavior
231 on a small foam ball (character size of $\sim 2 \text{ mm}$) has
232 been examined and experimentally observed, where the
233 particle is transversely trapped to the center of the field,
234 see Fig. 4(b). Here, the sample of the metastructure
235 is fabricated using a 3D printer (Wiiibox Four) with
236 the material PLA. The printing resolution is 0.1mm. A
237 signal generator (RIGOL DG1032) and a power amplifier
238 (CROWN XLi2500) are connected to a loudspeaker with
239 a rated power of 100 W (Lutiane DL-630). The working
240 frequency is 17 kHz, corresponding to the wavelength $\lambda \sim$

241 2 cm. The experimental diagram is shown in Fig. 4(c).
242 The loudspeaker is fixed for a 45-degree incidence to the
243 sample. An absorption panel is set at a specific position
244 to separate incident and reflected acoustic fields. The
245 acoustic fields are scanned in the target region with a
246 step of 0.5 cm. Then interpolation process is made on
247 the measured data. To better investigate the transverse
248 particle trapping, the foam is hanging by a light string
249 with a diameter of about 0.07 mm, and the particle can
250 move freely in the transverse direction.

251 IV. CONCLUSION

252 In summary, we have analyzed both on-axis and
253 off-axis particle trapping behaviors generated by finite
254 acoustic axisymmetric Bessel beams. The reversal of
255 the trapping behaviors on the beam axis has been
256 recovered when varying the paraxiality parameter β of
257 the Bessel beam. In addition, the applicable spatial
258 range for the approximated Bessel beam from a sound
259 source of finite size has been quantitatively investigated.
260 A lossy acoustic metastructure has been used for the
261 generation of zero-order Bessel beams, which are then
262 used to trap a small foam ball. Our work is beneficial to
263 the further development of simplified acoustic tweezers
264 using ordinary Bessel beams, which are desired for many
265 applications involving particle manipulations.

266 ACKNOWLEDGMENTS

267 This work was supported by the National Natural
268 Science Foundation of China (Grant No. 12204241
269 and No. 11974186), the Natural Science Foundation
270 of Jiangsu Province (Grant No. BK20220924 and No.
271 BK20200070), and the open research foundation of Key
272 Laboratory of Modern Acoustics, Ministry of Education,
273 Nanjing University.

274 X. F. and Y. Z. contributed equally to this work.

- [1] A. P. Sarvazyan, O. V. Rudenko, and W. L. Nyborg, “Biomedical applications of radiation force of ultrasound: historical roots and physical basis,” *Ultrasound in Medicine & Biology* **36**, 1379–1394 (2010).
- [2] L. P. Gor’kov, “On the forces acting on a small particle in an acoustical field in an ideal fluid,” *Sov. Phys. Dokl.* **6**, 773 – 775 (1962).
- [3] J. Wu, “Acoustical tweezers,” *J. Acoust. Soc. Am.* **89**, 2140–2143 (1991).
- [4] P. L. Marston, “Axial radiation force of a Bessel beam on a sphere and direction reversal of the force,” *J. Acoust. Soc. Am.* **120**, 3518–3524 (2006).
- [5] L. K. Zhang and P. L. Marston, “Geometrical interpretation of negative radiation forces of acoustical Bessel beams on spheres,” *Phys. Rev. E* **84**, 035601 (2011).
- [6] L. K. Zhang and P. L. Marston, “Axial radiation force exerted by general non-diffracting beams,” *J. Acoust. Soc. Am.* **131**, EL329–EL335 (2012).
- [7] S. Xu, C. Qiu, and Z. Liu, “Transversally stable acoustic pulling force produced by two crossed plane waves,” *Europhys. Lett.* **99**, 44003 (2012).
- [8] C. R. P. Courtney, B. W. Drinkwater, C. E. M. Demore, S. Cochran, A. Grinenko, and P. D. Wilcox, “Dexterous manipulation of microparticles using Bessel-function acoustic pressure fields,” *Appl. Phys. Lett.* **102**, 123508 (2013).
- [9] C. E. M. Démoré, P. M. Dahl, Z. Yang, P. Glynne-Jones, A. Melzer, S. Cochran, M. P. MacDonald, and G. C. Spalding, “Acoustic tractor beam,” *Phys. Rev. Lett.* **112**, 174302 (2014).
- [10] A. Marzo, S. A. Seah, B. W. Drinkwater, D. R. Sahoo, B. Long, and S. Subramanian, “Holographic acoustic elements for manipulation of levitated objects,” *Nature communications* **6**, 8661 (2015).
- [11] K. Melde, A. G. Mark, T. Qiu, and P. Fischer, “Holograms for acoustics,” *Nature* **537**, 518–522 (2016).
- [12] A. Marzo, A. Ghobrial, L. Cox, M. Caleap, A. Croxford, and B. W. Drinkwater, “Realization of compact tractor beams using acoustic delay-lines,” *App. Phys. Lett.* **110**, 014102 (2017).
- [13] A. Marzo, M. Caleap, and B. W. Drinkwater, “Acoustic virtual vortices with tunable orbital angular momentum for trapping of mie particles,” *Phys. Rev. Lett.* **120**, 044301 (2018).
- [14] L. K. Zhang, “Reversals of orbital angular momentum transfer and radiation torque,” *Phys. Rev. Applied* **10**, 034039 (2018).
- [15] X. D. Fan and L. K. Zhang, “Trapping force of acoustical Bessel beams on a sphere and stable tractor beams,” *Phys. Rev. Applied* **11**, 014055 (2019).
- [16] X.-D. Fan and L. Zhang, “Phase shift approach for engineering desired radiation force: Acoustic pulling force example,” *The Journal of the Acoustical Society of America* **150**, 102–110 (2021).
- [17] N. Korozlu, A. Biçer, D. Sayarcan, O. A. Kaya, and A. Cicek, “Acoustic sorting of airborne particles by a phononic crystal waveguide,” *Ultrasonics* **124**, 106777 (2022).
- [18] D. B. Thiessen, L. K. Zhang, and P. L. Marston, “Radiation force on spheres in helicoidal Bessel beams modeled using finite elements,” *J. Acoust. Soc. Am.* **125**, 2552 (2009).
- [19] D. Baresch, J. L. Thomas, and R. Marchiano, “Three-dimensional acoustic radiation force on an arbitrarily located elastic sphere,” *J. Acoust. Soc. Am.* **133**, 25–36 (2013).
- [20] G. T. Silva, J. H. Lopes, and F. G. Mitri, “Off-axial acoustic radiation force of repulsor and tractor Bessel beams on a sphere,” *IEEE Transactions on Ultrasonics, Ferroelectrics, and Frequency Control* **60**, 1207 – 1212 (2013).
- [21] Z. Liu, X. Zhang, Y. Mao, Y. Y. Zhu, Z. Yang, C. T. Chan, and P. Sheng, “Locally resonant sonic materials,” *Science* **289**, 1734–1736 (2000).
- [22] Y. Li, B. Liang, Z.-m. Gu, X.-y. Zou, and J.-c. Cheng, “Reflected wavefront manipulation based on ultrathin planar acoustic metasurfaces,” *Scientific reports* **3**, 1–6 (2013).
- [23] J. Zhao, B. Li, Z. Chen, and C.-W. Qiu, “Manipulating acoustic wavefront by inhomogeneous impedance and steerable extraordinary reflection,” *Scientific reports* **3**, 1–6 (2013).
- [24] P. Zhang, T. Li, J. Zhu, X. Zhu, S. Yang, Y. Wang, X. Yin, and X. Zhang, “Generation of acoustic self-bending and bottle beams by phase engineering,” *Nature communications* **5**, 1–9 (2014).
- [25] Y. Li, X. Jiang, R.-q. Li, B. Liang, X.-y. Zou, L.-l. Yin, and J.-c. Cheng, “Experimental realization of full control of reflected waves with subwavelength acoustic metasurfaces,” *Physical Review Applied* **2**, 064002 (2014).
- [26] K. Tang, C. Qiu, M. Ke, J. Lu, Y. Ye, and Z. Liu, “Anomalous refraction of airborne sound through ultrathin metasurfaces,” *Scientific reports* **4**, 1–7 (2014).
- [27] Y. Xie, W. Wang, H. Chen, A. Konneker, B.-I. Popa, and S. A. Cummer, “Wavefront modulation and subwavelength diffractive acoustics with an acoustic metasurface,” *Nature communications* **5**, 1–5 (2014).
- [28] Y. Li, X. Jiang, B. Liang, J.-c. Cheng, and L. Zhang, “Metascreen-based acoustic passive phased array,” *Physical Review Applied* **4**, 024003 (2015).
- [29] G. Ma and P. Sheng, “Acoustic metamaterials: From local resonances to broad horizons,” *Science advances* **2**, e1501595 (2016).
- [30] S. A. Cummer, J. Christensen, and A. Alù, “Controlling sound with acoustic metamaterials,” *Nature Reviews Materials* **1**, 1–13 (2016).
- [31] X. Zhu, K. Li, P. Zhang, J. Zhu, J. Zhang, C. Tian, and S. Liu, “Implementation of dispersion-free slow acoustic wave propagation and phase engineering with helical-structured metamaterials,” *Nature Communications* **7**, 1–7 (2016).
- [32] X. Jiang, Y. Li, B. Liang, J.-c. Cheng, and L. Zhang, “Convert acoustic resonances to orbital angular momentum,” *Physical review letters* **117**, 034301 (2016).
- [33] X.-D. Fan, Y.-F. Zhu, B. Liang, J. Yang, and J.-C. Cheng, “Broadband convergence of acoustic energy with binary reflected phases on planar surface,” *Applied Physics Letters* **109**, 243501 (2016).

- [34] Y. Zhu, X. Fan, B. Liang, J. Cheng, and Y. Jing, "Ultrathin acoustic metasurface-based schroeder diffuser," *Physical Review X* **7**, 021034 (2017).
- [35] Y. Li, C. Shen, Y. Xie, J. Li, W. Wang, S. A. Cummer, and Y. Jing, "Tunable asymmetric transmission via lossy acoustic metasurfaces," *Physical review letters* **119**, 035501 (2017).
- [36] Y. Zhu, J. Hu, X. Fan, J. Yang, B. Liang, X. Zhu, and J. Cheng, "Fine manipulation of sound via lossy metamaterials with independent and arbitrary reflection amplitude and phase," *Nature communications* **9**, 1–9 (2018).
- [37] B. Assouar, B. Liang, Y. Wu, Y. Li, J.-C. Cheng, and Y. Jing, "Acoustic metasurfaces," *Nature Reviews Materials* **3**, 460–472 (2018).
- [38] X.-D. Fan, B. Liang, J. Yang, and J.-C. Cheng, "Illusion for airborne sound source by a closed layer with subwavelength thickness," *Scientific reports* **9**, 1–6 (2019).
- [39] X.-D. Fan and L. Zhang, "Acoustic orbital angular momentum hall effect and realization using a metasurface," *Physical Review Research* **3**, 013251 (2021).
- [40] S. Zhang, C. Xia, and N. Fang, "Broadband acoustic cloak for ultrasound waves," *Physical review letters* **106**, 024301 (2011).
- [41] X. Zhu, B. Liang, W. Kan, X. Zou, and J. Cheng, "Acoustic cloaking by a superlens with single-negative materials," *Physical review letters* **106**, 014301 (2011).
- [42] X. Jiang, B. Liang, X.-y. Zou, L.-l. Yin, and J.-c. Cheng, "Broadband field rotator based on acoustic metamaterials," *Applied physics letters* **104**, 083510 (2014).
- [43] W. Kan, B. Liang, R. Li, X. Jiang, X.-y. Zou, L.-l. Yin, and J. Cheng, "Three-dimensional broadband acoustic illusion cloak for sound-hard boundaries of curved geometry," *Scientific reports* **6**, 1–8 (2016).
- [44] H. Gao, Y.-f. Zhu, X.-d. Fan, B. Liang, J. Yang, and J.-C. Cheng, "Non-blind acoustic invisibility by dual layers of homogeneous single-negative media," *Scientific reports* **7**, 1–7 (2017).
- [45] S. Inoue, S. Mogami, T. Ichiyama, A. Noda, Y. Makino, and H. Shinoda, "Acoustical boundary hologram for macroscopic rigid-body levitation," *The Journal of the Acoustical Society of America* **145**, 328–337 (2019).
- [46] Y. Zhu and B. Assouar, "Systematic design of multiplexed-acoustic-metasurface hologram with simultaneous amplitude and phase modulations," *Physical Review Materials* **3**, 045201 (2019).
- [47] Y. Zhu, N. J. Gerard, X. Xia, G. C. Stevenson, L. Cao, S. Fan, C. M. Spadaccini, Y. Jing, and B. Assouar, "Systematic design and experimental demonstration of transmission-type multiplexed acoustic metaholograms," *Advanced Functional Materials* **31**, 2101947 (2021).
- [48] G. Ward, R. Lovelock, A. Murray, A. P. Hibbins, J. R. Sambles, and J. Smith, "Boundary-layer effects on acoustic transmission through narrow slit cavities," *Physical review letters* **115**, 044302 (2015).
- [49] M. Molerón, M. Serra-Garcia, and C. Daraio, "Visco-thermal effects in acoustic metamaterials: from total transmission to total reflection and high absorption," *New Journal of Physics* **18**, 033003 (2016).